J. Micromech. Microeng. 1 (1991) 60–65. Printed in the UK

# Fabrication and testing of a microdynamic rotor for blood flow measurements

**S D Rapoport†, M L Reed† and L E Weiss‡**

†Department of Electrical and Computer Engineering, Carnegie Mellon University, Pittsburgh, PA 15213, USA
‡Robotics Institute, Carnegie Mellon University, Pittsburgh, PA 15213, USA

Received 15 October 1990, accepted for publication 1 December 1990

**Abstract.** Flow studies have been conducted, *in vitro*, on prototype microfabricated blood flow sensors. The envisioned measurement principle is the detection of the rotation of a micromachined polysilicon rotor of diameter 300 $\mu$m. Repeatable rotation rates as a function of media velocity were obtained for both nitrogen and water. Fluid flow asymmetries, necessary to produce a torque on the rotor, were created by integrating a 2 $\mu$m thick polysilicon cap over half the rotor. Blade deflection, due to intrinsic stress in the polysilicon films, was eliminated by thermal annealing. This allows the rotor, 2 $\mu$m thick, to rotate in the 7 $\mu$m gap between the substrate and the polysilicon cap. Operation of the device in heparinized dog blood resulted in considerable numbers of erythrocytes sticking to the polysilicon elements.

## 1. Introduction

The purpose of this research was to design and fabricate an *in vivo* flow sensor to measure blood velocity in coronary arteries. The possibility of approaching this application with microdynamic tools was motivated by recent developments in silicon micromachining, [1–6]. The envisaged use of this sensor is to measure arterial blood velocity to determine the efficacy of balloon catheterization (angioplasty) or other methods of unblocking clogged arteries.

Angioplasty is a non-surgical technique for reversing arterial stenosis, and is an important alternative to more traditional methods such as bypass surgery. Arterial stenosis is the occlusion of an artery, and is caused by plaque build-up on the arterial walls. In angioplasty, a deflated balloon on the end of a guide wire is inserted into the stenosed area of an artery, and the balloon is inflated in the clogged area. The result is a stretched artery, which, when successful, allows blood to flow more freely [7, 8]. To determine if the angioplasty is successful, an absorptive dye is injected into the bloodstream while the patient is illuminated with x-rays. Stenosis is readily observed as an obstruction to the fluid flow. This method has several disadvantages, chief among which is that it cannot be used in vessels smaller than about 1 cm in diameter. Also, dye injection gives only qualitative information about the blood flow, and is painful due to the local heating arising from the x-ray absorption.

As an alternative, we have investigated the use of a microdynamic rotor as a sensing device. The potential of microdynamics technology for medical and surgical equipment, and in scientific instrumentation, is enormous. As yet, there are few demonstrated applications for the new technology. The goal of this study was to investigate some of the practical impediments to employing microdynamics in a useful medical application.

Two prototype blood flow sensors were designed and fabricated from polysilicon thin films. Both devices incorporated a rotor with a diameter of 300 $\mu$m. To keep the rotor fixed to the silicon substrate, but to allow it to rotate, a center shaft and hub were designed using techniques described elsewhere [4]. The first design has flow channel walls to guide the fluid across the rotor blade, causing a velocity gradient which is necessary to make the rotor turn. The second device incorporates a semicircular cap covering half the rotor, giving rise to asymmetrical forces on the rotor. The flow sensors were tested in nitrogen, air, water, and blood; rotation rates were calibrated as a function of medium velocity in both nitrogen and water.

## 2. Device and process design

The fabrication sequence of the micromechanical rotor structure followed the process described by Fan [4] for micromachining detachable moving parts on silicon substrates. The basis for fabrication of movable parts is the use of sacrificial layers that act both as spacers and also to keep the parts attached to the wafer during fabrication. The process used in this project deviated

0960-1317/91/01060+06 $3.50 © 1991 IOP Publishing Ltd

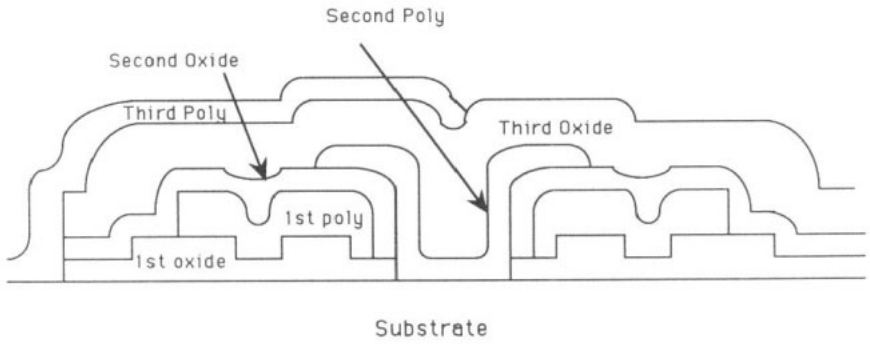


**Figure 1.** Schematic cross section of the polysilicon and $SiO_2$ layers comprising the device, before the sacrificial oxide etch.

from previously published processes by employing wet chemical etching exclusively.

A schematic cross section of the device, before the final sacrificial oxide etch, is shown in figure 1. The mask patterns (six levels) are shown in figure 2. The process begins with a (100)-oriented silicon substrate, onto which 2.0 $\mu$m of $SiO_2$ is deposited, using a plasma-enhanced chemical vapor deposition system. After a masking step to define a small-area bushing region, the rotor film was deposited, a 2.0 $\mu$m layer of polysilicon. Subsequent layers of $SiO_2$ and polysilicon were similarly deposited to form the sacrificial layers, the axle and hub, and the semicircular rotor cap. The lithographic processes defines a conformal, self-aligned bearing between the hub and rotor [9]. The lip of the second polysilicon layer, which extends over the inner diameter of the rotor, restrains the rotor from detaching. After patterning the third polysilicon layer, the sacrificial $SiO_2$ films are removed in hydrofluoric acid. This releases the rotor and allows it to turn.

We experimented with two designs of the rotor. The first design, which we will refer to as the four-mask version, did not include the final $SiO_2$ or polysilicon layers. The second design, which used the full six-mask process, included the semicircular cap over half the rotor. Electron micrographs of the two designs, after the sacrificial $SiO_2$ etch, are shown in figures 3 and 4. Means for relaying the rotation rate information off the device were not included with these designs, as the primary goal was to investigate the interactions of the rotor itself with a moving fluid.

## 3. Stress reduction in polysilicon films

The high-temperature chemical vapor deposition processes used to deposit the polysilicon films result in a significant amount of residual stress [10–16]. The stress can be observed as a bowing in the polysilicon flanges of the rotor, after the final sacrificial etch. Figure 3 shows the upward bending of the rotor flanges for a device built with the simpler four-mask process. The residual stress in

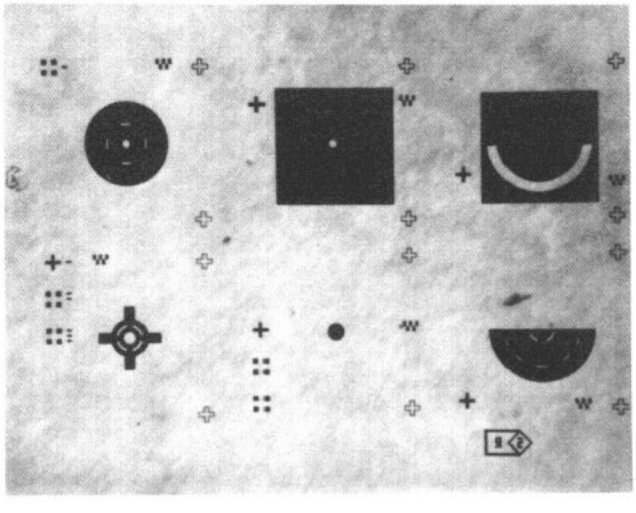

**Figure 2.** Mask patterns. The upper patterns are oxide cuts; the lower define polysilicon structures. The rotor itself is defined by the pattern in the lower left; the one in the lower right defines the semicircular cap (third polysilicon layer) which covers half the rotor.

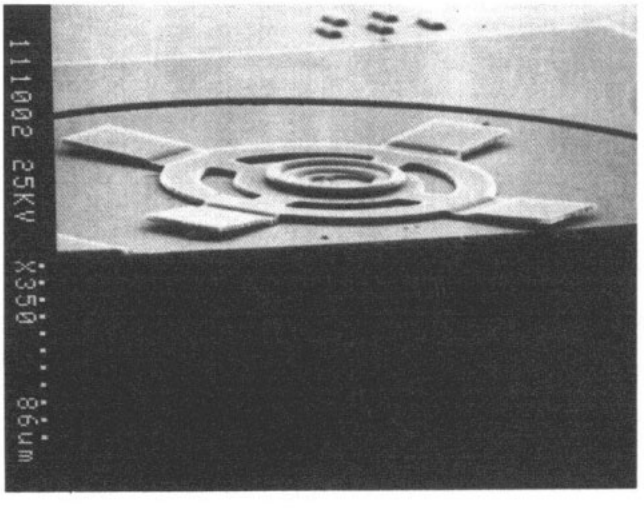


**Figure 3.** Device fabricated with four-mask process (without cap), after sacrificial oxide etch. Stress in unannealed polysilicon layers results in upward bending of rotor arms.

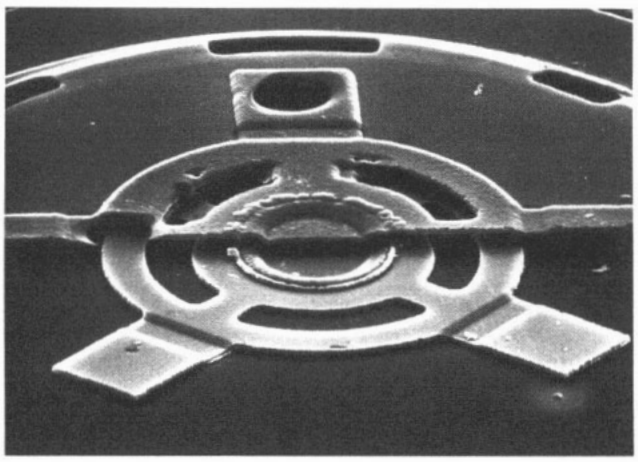

**Figure 4.** Device fabricated with six-mask process, after sacrificial oxide etch.

the polysilicon has two components: a compressive stress due to a difference in the thermal expansion coefficients at the polysilicon-$SiO_2$ interface, and a residual tensile stress due to a gradient in poly-grain size as a function of thickness.

The coefficient of thermal expansion of polysilicon is a factor of 6 greater than that of $SiO_2$ [17]. Therefore, when the polysilicon cools after the deposition (from 625°C to 25°C), the material at the polysilicon-$SiO_2$ interface cannot contract as much as the material in the bulk of the rotor. This leaves strain that makes the rotor flanges bend when the $SiO_2$ is etched away. In the four-mask process this does not cause a problem. However, in the six-mask process the upward bending would cause the rotor flanges to press against the underside of the semicircular cap, preventing rotation of the rotor.

The film stress can be reduced by thermal annealing [10]. A mask pattern was designed to find satisfactory anneal conditions for the polysilicon films. A series of 2.0 $\mu$m thick free-standing cantilevers and doubly supported beams (bridges) of different widths and lengths were fabricated. The deflection of the cantilevers and the buckling of the bridge structures were observed using an electron microscope after the sacrificial oxide etch. For example, an unannealed cantilever, 150 $\mu$m long, deflected by over 5 $\mu$m. We found that annealing the films at 1100°C for 30 minutes (in nitrogen) reduced the beam deflection to negligible levels. This anneal step was incorporated into the six-mask process, just before the sacrificial oxide etch. This allows the 2 $\mu$m thick rotor to turn in the 7 $\mu$m gap between the substrate and the polysilicon cap without binding.

The anneal step gave rise to a process anomaly which can be seen in figure 4. Large holes, up to 50 $\mu$m in diameter, are observed in random locations in the third polysilicon film. These perforations did not occur on unannealed samples. It appears that impurities at the upper $SiO_2$-polysilicon interface may have undergone a reaction during the (relatively high-temperature) anneal step; evolution of gas phase reaction products then 'blew off' portions of the polysilicon film, leaving behind the crater-like structures seen in figure 4. (Bubbling of phosphosilicate glass films, due to a reaction between the phosphorus and adsorbed water, has been observed during high-temperature reflow annealing [18].

## 4. Fluid flow experiments

To characterize the performance of the device, we measured the rotation rate of the rotor as a function of fluid velocity. The devices were affixed with a silicone rubber compound to square-cross-section glass tubes (1.5 mm OD). This tube, with the sample mounted at the end, was then inserted into a larger (2 mm OD) glass tube. The entire assembly was observed with an optical microscope. (Square-cross-section tubing was used to reduce the optical distortion characteristic of round tubes.) The microscope illuminator was replaced by a stroboscope to freeze the motion of the rotor; in this way, the rotation rate was obtained. Flexible tubing was attached to both ends of the larger square capillary tube. Fluids were run through the tubing from a pressurized canister filled with the air, nitrogen, water, or blood.

The rotors fabricated with the integral polysilicon caps exhibited very high starting torques and thus did not rotate freely in moving fluids. The rotors were fully released from the substrate, and could be turned manually with a wire, but they did not perform sufficiently well to make quantitative measurements of rotation rate. The results presented here are for devices fabricated without the integral cap. Shear gradients were introduced with liquid media by manually affixing a glass plate over half the rotor; however, this was not necessary for operation in gases.

The fluid flow experiments were all conducted with isobaric conditions upstream of the rotor. The flow velocity was controlled by a throttle valve approximately 30 cm downstream of the device. These conditions approximate the situation in a blocked artery, where the pressure is relatively constant during a heartbeat, but the flow velocity is determined by the throttling effect of an occlusion. The flow velocity was calibrated by timing the displacement of a known quantity of gas or liquid.

Typical results are shown in figures 5 and 6, which show rotation rates, in rotations per minute, as a function of nitrogen and water velocity in $m\,s^{-1}$. The vertical error bars represent the uncertainty in the rotation rate of about $\pm 70$ rpm; this was the range over which the strobe frequency could be varied without a significant change in the image of the frozen rotor. The full lines are least-square linear fits to the data. We observe a strong correlation for both fluids: the correlation coefficients are $r^2 = 0.72$ (nitrogen) and 0.90 (water). Also apparent from the graphs is the requirement for a finite starting torque before the rotor begins turning. Consistent operation of the rotor was not possible below a minimum fluid velocity. We believe this starting torque arises from static friction between the rotor bearing and axle. Contact

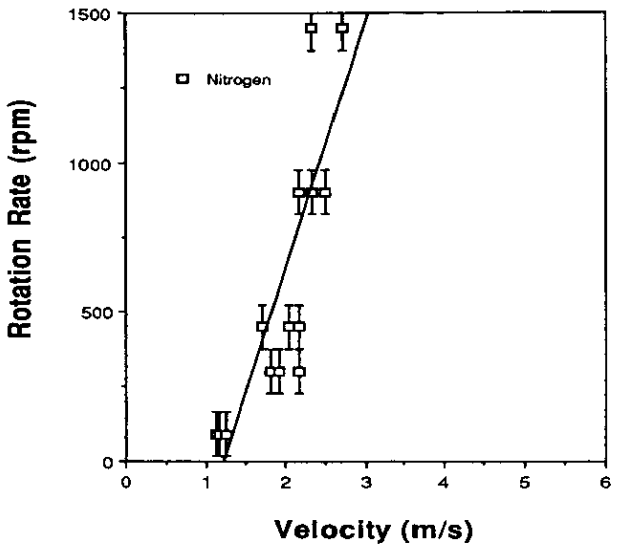


**Figure 5.** Rotation rate (rpm) versus nitrogen velocity ($ms^{-1}$).

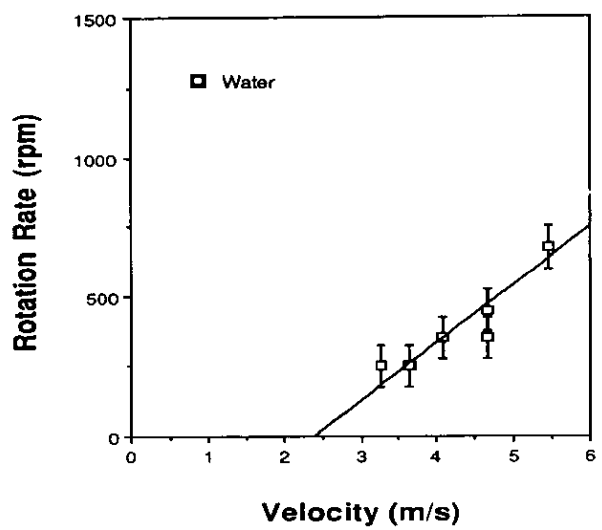


**Figure 6.** Rotation rate (rpm) versus water velocity ($ms^{-1}$).

between the bushings and substrate is not thought to contribute significantly to the friction. We base this assertion on two observations: (1) the rotor would generally lift out of its equilibrium plane before for flow velocities lower than the minimum necessary for rotation; (2) operation of the rotor for extended times (over 100 hours) resulted in no visible wear of the substrate beneath the bushings.

The fluid flow for the experiments in water was laminar. Taking the characteristic distance of the system, $D$, to be the fluid thickness above the rotor, the Reynolds number

$$\mathrm{Re} = \rho v D/\mu$$

where $\rho$, $v$, and $\mu$ are the fluid density, velocity, and viscosity, is $\mathrm{Re} \approx 4000$, well within the laminar regime [19]. An estimate of the boundary layer thickness $\delta$ can be obtained from

$$\delta = \sqrt{xD/\mathrm{Re}}$$

where the $x$ represents the distance from the leading-edge obstruction to the rotor, about 2 mm. This yields a boundary layer thickness of approximately 30 $\mu$m, which is over an order of magnitude greater than the rotor thickness. The picture one obtains from these calculations is of a thin rotor, slowly propelled by torque resulting from viscous drag of the fluid.

Naturally, the fluid dynamics is considerably more intricate than this simple description. For example, during our experiments using compressed air as the fluid, we observed a peculiar effect as the air passed over the leading edge of the die boundary. Water vapor in the air supply condensed on the silicon surface and could be observed as interference fringes; typical thicknesses were less than 1 $\mu$m. The downstream edge of the water film (about 20 to 40 $\mu$m from the die edge) exhibited a sinusoidal shape, with the peak and valley locations perpendicular to the flow direction. The shape of the water film was not stationary, even with no change in flow parameters. The sinusoidal trailing edge was observed to oscillate, apparently from micro-turbulences created by the presence of the polysilicon films. The oscillation rate (several Hz) was too rapid to have any discernible effect on the rotor movement.

One might expect that the response of the device in blood would be different than in water. The viscosity of plasma is only slightly greater than water, but blood contains a great deal of solid material in suspension which could impart momentum impulses to the rotor. We attempted to operate the devices by passing dog blood through the capillary tube. The blood contained two anti-coagulants, heparin and citrate dextrose, to prevent clotting and subsequent clogging of the device. As of this writing, we have not been able to make quantitative measurements of the rotation rate using blood as the fluid medium. The chief difficulty is the opacity of the blood. Although the distance between the rotor and the inside of the glass tube is only 1.2 mm, observation of the rotor through this thickness of blood is difficult. Partial dilution of the blood with deionized water did not alleviate this problem.

Qualitative observations of the interaction of the device with blood are depicted in the micrographs of figures 7 and 8. After immersion in flowing blood, the devices were rinsed in water to remove the excess fluid, and then coated with approximately 50 Å of gold to facilitate imaging in the electron microscope. The round features are erythrocytes that have stuck to the device; they range from 5 $\mu$m to 7 $\mu$m in diameter. These micrographs point up a potentially serious problem applicable to any microdynamic device placed in the bloodstream. The erythrocytes tend to stick to the rough surface of the polysilicon, much more than to the smoother substrate surface. (It should be noted that no special attempt was made to engineer a smooth surface for the polysilicon films; smoother films can certainly be deposited with

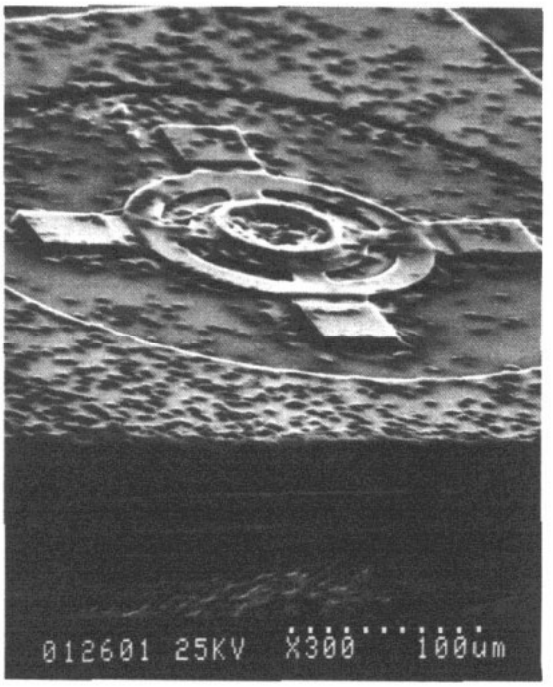


**Figure 7.** Rotor after testing in blood. The erythrocytes, approximately 6 $\mu$m in diameter, are seen as round flat discs adhering to the device.

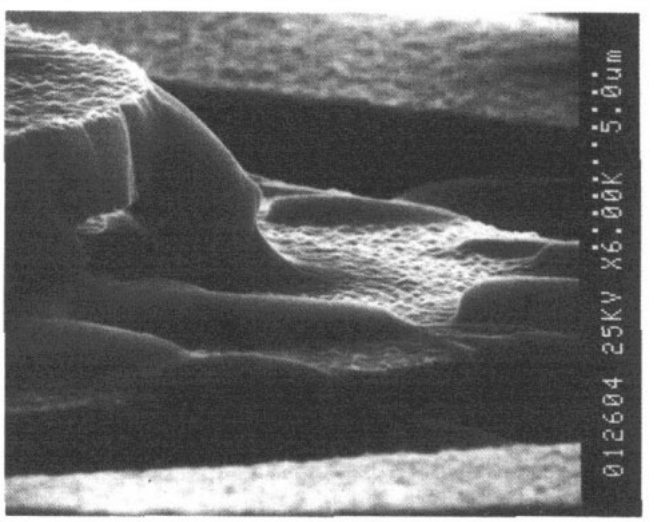


**Figure 8.** Close-up of rotor axle and hub, after operation in blood.

current vapor deposition technology. However, annealing for stress reduction tends to roughen the surface of even very smooth films, so this problem is likely to be of general concern.) Also, the thickness of the erythrocytes is comparable to the gap between the device films, which opens up the possibility of cellular material jamming the rotor.

The minimum liquid velocity for rotor operation was approximately 300 cm s$^{-1}$. This value is substantially greater than the typical blood velocity in major coronary arteries, about 20 cm s$^{-1}$ during the systolic pulsation. Clearly, much needs to be done to reduce the starting torque before this approach would find clinical application. However, it is encouraging that even with the artificially high fluid velocities, the devices were quite robust and unbreakable. This is a major consideration in placing microdynamic elements in the vascular system, since emboli migrating downstream can block other vessels and initiate cerebral apoplexy.

## 5. Magnetoresistance sensing of rotation rate

A useful sensor must have a transduction mechanism to transform the rotor rotation rate into an electrical signal. In macroscopic machines with rotating elements, brushes or cam/armature assemblies are often used to as an interface between the rotating and stationary portions of the system. However, the physical coupling inherent in this approach would introduce serious complexities in a microdynamic system. Non-contacting transduction mechanisms would have the advantage of reducing frictional drag on the moving parts, and would also be expected to be more reliable.

We propose the use of a magnetoresistive sensing element as a non-contacting coupling technique. Consider a rotor fabricated from a hard magnetic material, such as Ni/Co, with an in-plane uniaxial magnetization. As the rotor turns, the field from this microscopic permanent magnet will modulate the resistance of a bar of low-coercivity material such as permalloy (Fe/Ni) placed nearby, close to the rotor flanges. The change in resistivity provides an electrical signal, the frequency of which is proportional to the rotation rate, and hence the blood velocity. Note that, unlike a magnetic circuit which detects the rate of change of the magnetic flux through a closed loop, the magnetoresistive signal amplitude is independent of the relative velocity; thus the signal-to-noise ratio is largely independent of the rotation rate.

The maximum fractional change in resistivity, about 3%, will occur when the magnetic field intensity in the magnetoresistor reaches approximately 4 Oe. As a worst-case analysis, we consider the rotor to be a dipole. The magnetic field intensity $H$ is given by

$$H = M_s V/2\pi\mu_0 r^3$$

where $M_s$ is the saturation magnetization of the rotor, $V$ is the volume of the magnet, $\mu_0$ is the permeability, and $r$ is the distance from the center of the rotor to the magnetoresistor [20]. $M_s$ is approximately 500 emu cm$^{-3}$ for sputtered Ni/Co films; the rotor can be idealized as a bar magnet of volume $V = 50\,\mu\text{m} \times 300\,\mu\text{m} \times 2\,\mu\text{m}$; $r$ is slightly greater than the rotor radius of 150 $\mu$m. This gives $H \approx 8$ Oe, twice the value needed to produce the maximum resistance change in the magnetoresistive sensing element.

This first-order calculation confirms the utility of using a magnetized rotor, modulating the magnetoresistance of a nearby element, to sense the rotation rate.

Thin-film technologies for this approach are well established (e.g., thin-film magnetic recording heads); thus, no special difficulties are expected to arise from this combination of materials.

## 6. Summary

We have fabricated and tested prototype blood flow sensors utilizing silicon microfabrication technology. The objective was to examine the feasibility of a mechanical microrotor sensitive to the velocity of blood in coronary arteries, with eventual application to clinical monitoring of arterial blood velocity after angioplasty. A three-polysilicon-layer process, in which the rotor turns between the substrate and a semicircular cap, was developed to fabricate the microdynamic device. Annealing of the structure, before etching of the sacrificial $SiO_2$, resulted in planar polysilicon elements. Repeatable rotation rates in flowing fluids were obtained, and qualitative observations concerning operation of the device in blood were noted. A novel transduction method, based on the magnetoresistance of permalloy, was shown to be feasible for relaying the rotation rate information from the device.

## Acknowledgments

The authors wish to thank M Wholey, W Novogradac, M Mehregany, C Bowman, T Russell, and M Nagurka for many stimulating discussions. This research was supported by Shadyside Hospital (Pittsburgh) and the National Science Foundation.

## References

[1] Senturia S D 1989 *IEDM Tech. Digest* **89** 3
[2] Delapierre G 1989 *Sensors Actuators* **17** 123–38
[3] Petersen K E 1982 *Proc. IEEE* **70** 420–55
[4] Fan L-S, Tai Y-C and Muller R S 1988 *IEEE Trans. Electron Devices* **35** 724–30
[5] Parameswaran M, Baltes H P, Ristic L, Dhaded A C and Robinson A M 1989 *Sensors Actuators* **19** 289–307
[6] Trimmer W S N 1989 *Sensors Actuators* **19** 267–87
[7] Ishinger T 1986 *Practice of Coronary Angioplasty* (Berlin: Springer)
[8] Dotter C T, Gruntzig A R, Schoop W and Zeitler E (ed.) 1983 *Percutaneous Transluminal Angioplasty* (Berlin: Springer)
[9] Mehregany M 1989 private communication
[10] Guckel H, Burns D W, Visser C C G, Tilmans H A C and Deroo D 1989 *IEEE Trans. Electron Devices* **35** 800–1
[11] Howe R T 1985 *Micromachining and Micropackaging of Transducers* ed Fung C D Cheung P W, Ko W H and Fleming D G (Amsterdam: Elsevier) pp 169–87
[12] Howe R T and Muller R S 1983 *J. Appl. Phys.* **54** 4674–5
[13] Mehregany M, Howe R T and Senturia S D 1987 *J. Appl. Phys.* **62** 3579–84
[14] Guckel H, Randazzo T and Burns D W 1985 *J. Appl. Phys.* **57** 1671–5
[15] Yang K L, Wilcoxen D and Gimpelson G 1989 *Micro Electro Mechanical Systems (Salt Lake City, UT 1989)* (Piscataway, NJ: IEEE)
[16] Kamins T 1988 *Polycrystalline Silicon for Integrated Circuit Applications* (Norwell, MA: Kluwer-Academic)
[17] Riethmuller W and Benecke W 1988 *IEEE Trans. Electron Devices* **35** 758–63
[18] Reed M 1982 unpublished results
[19] Shames I H 1962 *Mechanics of Fluids* 2nd edn (New York: McGraw-Hill)
[20] Chikazumi S 1964 *Physics of Magnetism* (Malabar, FL: Krieger)